

Molecular mechanics and dynamics simulation of hydrogen diffusion in aluminum melt

Huo-sheng Wang^{1,2}, *Gao-sheng Fu¹, Chao-zeng Cheng¹, Li-li Song¹ and Lian-deng Wang³

1. School of Materials Science and Engineering, Fuzhou University, Fuzhou 350118, China

2. School of Materials Science and Engineering, Fujian University of Technology, Fuzhou 350118, China

3. School of Mechanical Engineering and Automation, Fuzhou University, Fuzhou 350118, China

Abstract: The main impurities in aluminum melt are hydrogen and Al_2O_3 , which can deteriorate melt quality and materials performance. However, the diffusion process of H atoms in aluminum melt and the interactions among Al atoms, Al_2O_3 and hydrogen have been studied rarely. Molecular mechanics and dynamics simulations are employed to study the diffusion behaviors of different types of hydrogen, such as free H atoms, H atoms in H_2 and H^+ ions in H_2O using COMPASS force field. Correspondingly, force field types h, h1h and h1o are used to describe different types of hydrogen which are labeled as H_h , H_{h1h} and H_{h1o} . The results show that the adsorption areas are maximum for H_{h1o} , followed by H_{h1h} and H_h . The diffusion ability of H_{h1o} is the strongest whereas H_h is hard to diffuse in aluminum melt because of the differences in radius and potential well depth of various types of hydrogen. Al_2O_3 cluster makes the Al atoms array disordered, creating the energy conditions for hydrogen diffusion in aluminum melt. Al_2O_3 improves the diffusion of H_h and H_{h1o} , and constrains H_{h1h} which accumulates around it and forms gas porosities in aluminum. H_{h1o} is the most dispersive in aluminum melt, moreover, the distance of Al- H_{h1o} is shorter than that of Al- H_{h1h} , both of which are detrimental to the removal of H_{h1o} . The simulation results indicate that the gas porosities can be eliminated by the removal of Al_2O_3 inclusions, and the dispersive hydrogen can be removed by adsorption function of gas bubbles or molten fluxes.

Key words: hydrogen in aluminum melt; molecular mechanics simulation; molecular dynamics simulation; COMPASS; hydrogen diffusion

CLC numbers: TG146.21

Document code: A

Article ID: 1672-6421(2017)06-478-07

The harmfulness and sources of hydrogen in aluminum melt have been discussed in previous studies^[1-3]. It is known that hydrogen is decomposed from steams, such as air humidity, damp raw materials and tools. Steams will react with aluminum at high temperatures, and generate Al_2O_3 and H atoms in aluminum melt (and/or hydrogen in air). Furthermore, the hydrogen in air will be decomposed into H atoms and diffuse into aluminum melt if the temperature and partial pressure are high enough. Some investigations also showed that H atoms are decomposed into H^+ ions by contact potential when they are adsorbed on Al_2O_3 inclusions^[4].

The solubility and diffusion dynamics of hydrogen

in aluminum melt have been studied, for example, the measurement of hydrogen content^[5,6], solubility calculation of hydrogen in aluminum melts with different constituents by thermodynamics^[7,8], and mass transformation principles of hydrogen and gas porosities formation mechanism during solidification of aluminum^[9-13], based on which a series of technologies and equipment have been developed for degassing^[14], such as spin rotor degassing^[15-17], ultrasonic degassing^[18-20] and vacuum degassing^[21]. The investigations mentioned above mainly focused on the behaviors of hydrogen during degassing process, and there were few studies on how hydrogen diffuse into aluminum melt and on the distribution state of hydrogen besides some experiments in solid aluminum^[22-24]. Moreover, the interactions among Al atoms, Al_2O_3 and hydrogen also affect hydrogen diffusion significantly. It has been proved practically that Al_2O_3 inclusions promote hydrogen content in aluminum melt. Several mechanisms have been developed to explain the phenomenon^[4,25], including mechanical interaction, electrostatic force, adsorption, nucleation interface theory etc. Professor Kang from

* Gao-sheng Fu

Male, born in 1965, Ph.D., Professor. His research interests mainly focus on aluminum melt treatment technologies such as purification, modification and grain refinement, mechanical behaviors of materials deformation, and materials forming technologies.

E-mail: fugaosheng@fzu.edu.cn

Received: 2017-04-01; Accepted: 2017-09-08

Fuzhou University of China proposed the mutual parasitic mechanism^[26], based on which Professor Fu presented purification principle for aluminum melt that inclusions removal is more important than degassing and developing high-efficient synthetic technology of aluminum melt treatment which is verified by practices^[27]. However, thorough studies on the interaction mechanism between Al₂O₃ and hydrogen are limited by the difficulties of experimental testing in high temperature melt.

The development of molecular mechanics and dynamics simulation technology in recent years makes it possible to recognize the aluminum melt structure and hydrogen behavior on the atomic scale^[28-29]. The technology was employed to study the process of hydrogen diffusing into aluminum melt, in which the hydrogen was divided into three categories: generic H atoms, H atoms in H² and H⁺ ions in H₂O, and three different COMPASS force field types, such as h, h1h and h1o were used, respectively. Furthermore, the interactions among Al atoms, Al₂O₃ and hydrogen were studied on atomic scale.

1 Simulation methods

Molecular mechanics and dynamics simulations were carried out using Sorption and Forcite module of Materials Studio software, respectively. Initial structure model of pure aluminum containing 864 Al atoms and the cell dimensions were a=b=c=24.30Å and α=β=γ=90° [Fig. 1(a)]. The structure model with Al₂O₃ cluster was derived from Fig. 1(a) by replacing some Al atoms with O²⁻ and Al³⁺ [Fig. 1(b)]. COMPASS force field was employed and force field types for atoms or ions in melt are listed in Table 1. In order to distinguish hydrogen with different force field types, generic H atoms, H atoms in H₂ and H⁺ ions in H₂O were labeled as H_h, H_{h1h} and H_{h1o}, respectively.

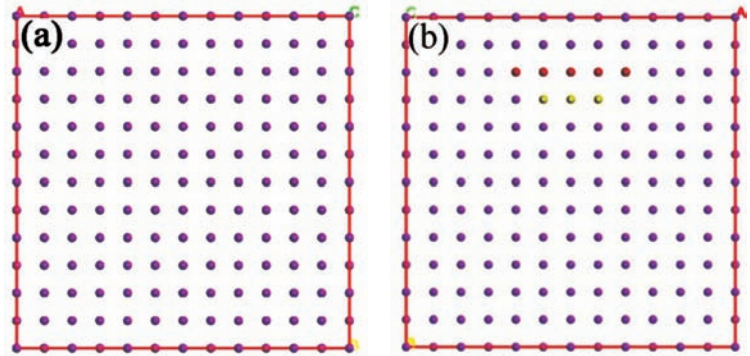


Fig. 1: Crystal structure of (a) pure aluminum and (b) aluminum containing Al₂O₃, in which purple atoms are Al, red atoms are O²⁻ and yellow atoms are Al³⁺

Table 1: Force field types of atoms or ions^[30]

Element	Al	Al ³⁺	O ²⁻	H	H	H ⁺
Force field type	al_m	al3o	o_al	h	h1h	h1o
Description	Aluminum in metal	Aluminum in oxides	Oxygen in Al ₂ O ₃	Generic hydrogen	Hydrogen in H ₂	Hydrogen bonded to O, F
Label in the paper	Al	Al ³⁺	O ²⁻	H _h	H _{h1h}	H _{h1o}

Molecular mechanics simulations were carried out using Metropolis method. The minimal energy aluminum melt structures and possible adsorption areas for different types of hydrogen were calculated, and average loading number was used to evaluate the adsorption capacity.

Molecular dynamics simulations were carried out at 1,023 K, the melting temperature of aluminum alloys. The calculations were run in NVT and NPT ensembles successively with a time step of 1 fs and a total simulation time of 50 ps. The control methods of temperature and pressure were NHL and Andersen, respectively. The simulation results were analyzed by radial distribution function (RDF), mean square displacement (MSD) and self-diffusion coefficient *D*, which was calculated by Einstein equation showed in Eq. (1)^[31,32].

$$D = \frac{1}{6} \lim_{t \rightarrow \infty} \frac{d}{dt} \langle [r_i(t) - r_i(0)]^2 \rangle \quad (1)$$

where $[r_i(t) - r_i(0)]^2$ is MSD, and $r_i(t)$ is the position of *i* atom at time of *t*.

The first-shell coordination number N_{ij} of H-H and Al-H was calculated by Eq.(2)^[33].

$$N_{ij} = 4\pi\rho_i \int_0^r g(r)r^2 dr \quad (2)$$

where N_{ij} is coordination number which subscript *i* is central atom and *j* is objective atom, ρ_i is numbers density of objective atoms, $g(r)$ is the value of RDF, and *r* is the cut-off distance.

2 Results and discussion

2.1 Aluminum melt structure at elevated temperature

Molecular dynamics simulation results of aluminum melt at elevated temperature are presented in Fig. 2. The pure aluminum melt (PAM) structure is similar to aluminum crystal that atoms array regularly [Fig. 2(a)]. This is consistent with literature^[24], in which the aluminum melt structure tested by XRD was similar to solid aluminum at a temperature below 1,670 K. RDF curves of Al-Al in aluminum melt at 1,023 K shown in Fig. 3 are also similar to those of solid aluminum^[34]. The first peak value of $g(r)$ is 3.50 at cut-off distance *r* of 0.289 nm, and there is obvious vibration attenuation for the curves. In aluminum melt containing Al₂O₃ (AMCO), Al atoms still array regularly besides those around the Al₂O₃ cluster [Fig. 2(b)], and the amplitude of RDF curve of AMCO is smaller than that of PAM, because

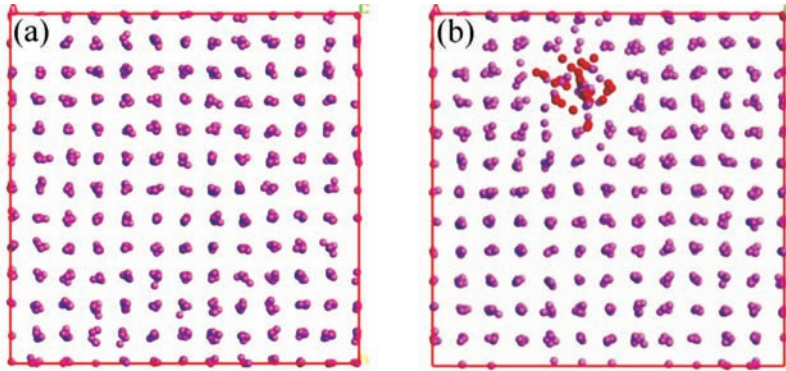


Fig. 2: Al atoms structure of (a) PAM and (b) AMCO at 1,023 K

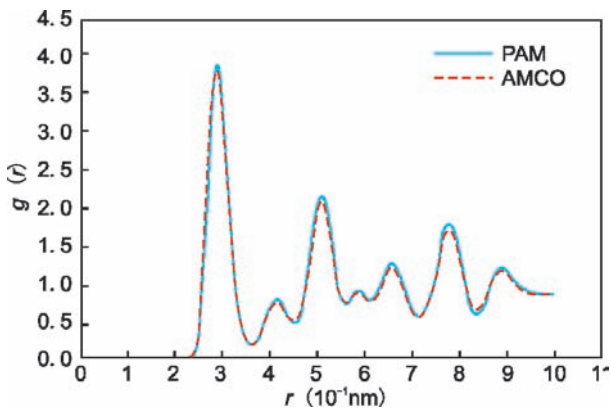


Fig. 3: RDF curves of Al-Al in aluminum melt at 1,023 K

Al_2O_3 increases the disorder degree of Al atoms array.

2.2 Possible adsorption areas for hydrogen in aluminum melt

The possible adsorption areas in aluminum melt for different types of hydrogen are shown in Fig. 4 and Fig. 5, and the average loading numbers are given in Table 2. H_h does not have any adsorption areas, and its average loading number is zero in PAM [Fig. 4(a)], but its adsorption area and average loading number increase slightly in AMCO [Fig. 5(a)]. The adsorption area of H_{h1h} in AMCO is more than that in PAM, and most of H_{h1h} are around Al_2O_3 cluster [Fig. 5(b)]. H_{h1o} has the biggest adsorption area and its average loading numbers are 6.98×10^{-3} and 7.97×10^{-3} in

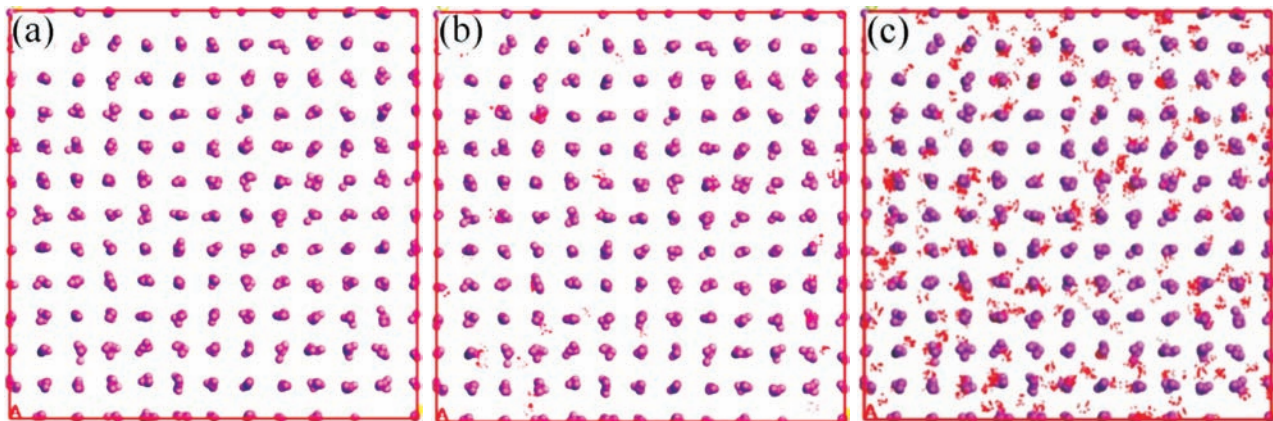


Fig. 4: Possible adsorption areas (displayed in red dots) in PAM for (a) H_h , (b) H_{h1h} and (c) H_{h1o}

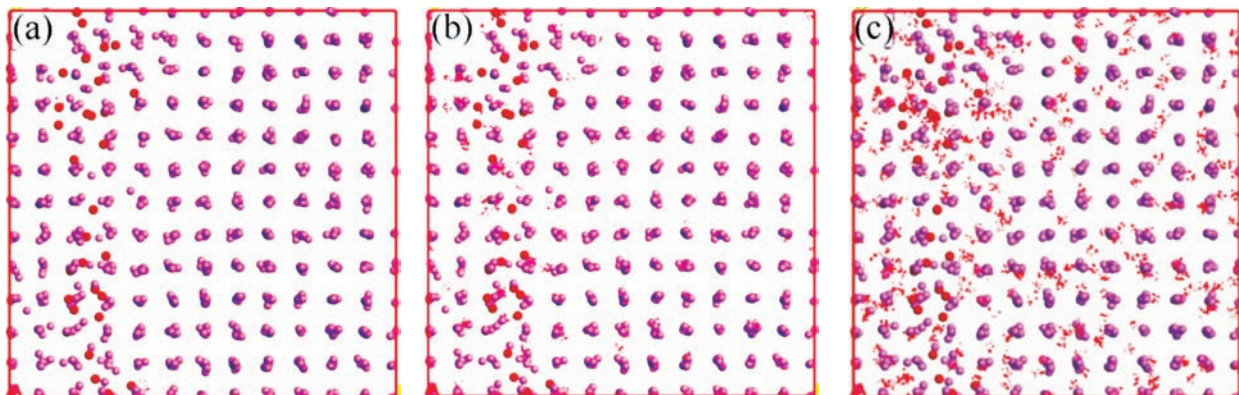


Fig. 5: Possible adsorption areas (displayed in red dots) in AMCO for (a) H_h , (b) H_{h1h} and (c) H_{h1o}

Table 2: Average loading numbers of different types of hydrogen in aluminum melt

Melt	PAM			AMCO		
Force field type	h	h1h	h1o	h	h1h	h1o
Average loading number	0	1.05×10^{-3}	6.98×10^{-3}	2.30×10^{-5}	1.67×10^{-3}	7.97×10^{-3}

PAM and AMCO, respectively, indicating that H_{h1o} can diffuse into aluminum melt most easily. Al_2O_3 cluster improves the adsorption for each type of hydrogen in aluminum melt.

2.3 Diffusion behaviors of H atoms in aluminum melt

2.3.1 Initial structure models of aluminum melt containing H atoms

Structure models of aluminum melt containing H atoms are presented in Fig. 6. These models were designed by displacing

50 Al atoms with H atoms in aluminum structures in Fig. 2. Force field types of h1, h1h and h1o were assigned to various types of hydrogen, respectively.

2.3.2 Diffusion of different types of hydrogen

The diffusion results of hydrogen in aluminum melt are shown in Fig. 7 and Fig. 8. In PAM, H_h diffuses slightly and keeps in cluster state, but H_{h1h} and H_{h1o} diffuse easily and H_{h1o} is more dispersive than H_{h1h} (Fig. 7). Moreover, Al_2O_3 improves the diffusion of H_h and H_{h1o} , but decreases the dispersion of H_{h1h} for the constraints

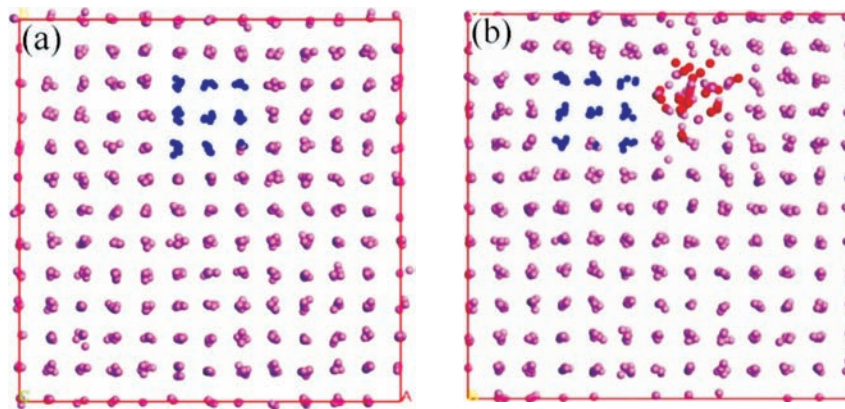


Fig. 6: Structure models of (a) PAM and (b) AMCO containing H atoms as shown in blue color

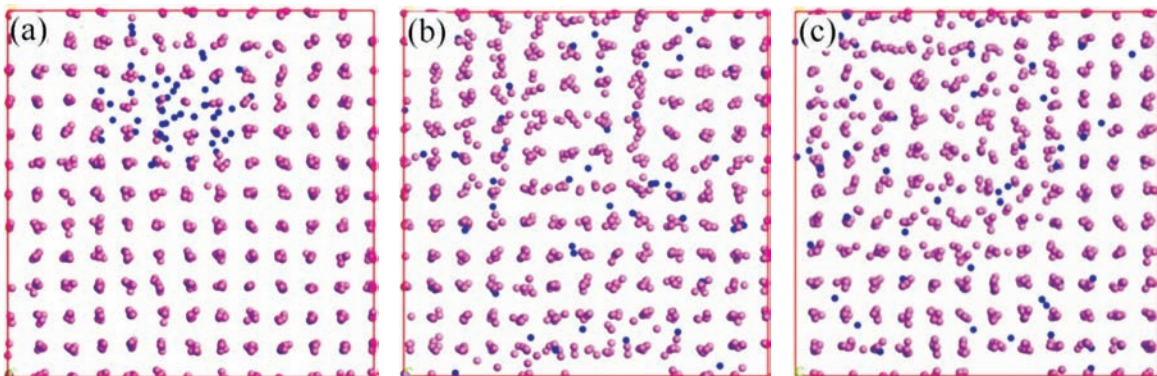


Fig. 7: Diffusion results of (a) H_h , (b) H_{h1h} and (c) H_{h1o} in PAM

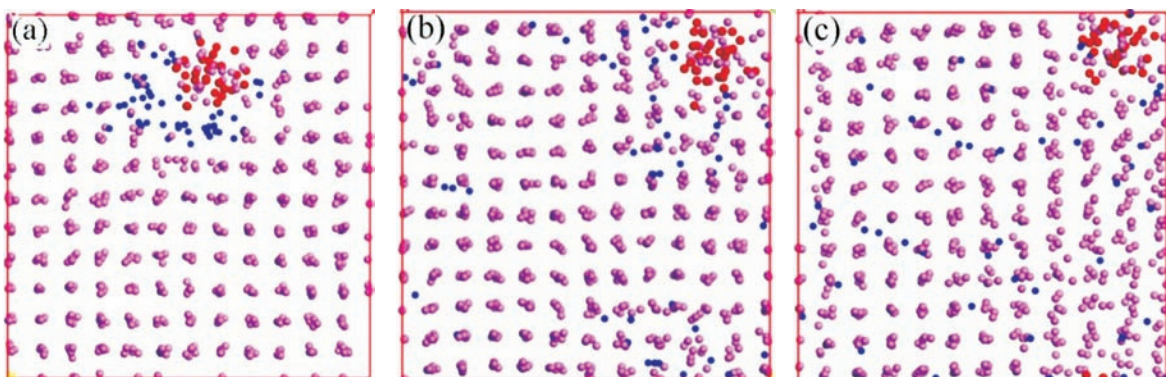


Fig. 8: Diffusion results of (a) H_h , (b) H_{h1h} and (c) H_{h1o} in AMCO

of Al_2O_3 cluster. The results are consistent with the molecular mechanics simulation results (Fig. 8).

The MSD curves are shown in Fig. 9, and the calculation results of self-diffusion coefficient D according to Eq. (1) are presented in Table 3. The D values of H_{h1o} are maximum, which are $9.03 \times 10^{-8} m^2 \cdot s^{-1}$ and $10.31 \times 10^{-8} m^2 \cdot s^{-1}$ in PAM and AMCO, respectively, and then followed by H_{h1h} and H_h . Al_2O_3 increases D values of H_h and H_{h1o} , but decreases those of H_{h1h} . The self-diffusion coefficient of H_{h1h} calculated in present work is consistent with that from experiments [25].

2.3.3 RDF curves of atoms or ions in aluminum melt

The RDF curves of H-H and Al-H are shown in Fig. 10 and Fig. 11, respectively, and the main data of the curves are given in Table 4, which are used to further study the interactions among Al atoms, Al_2O_3 and hydrogen in aluminum melt during diffusion.

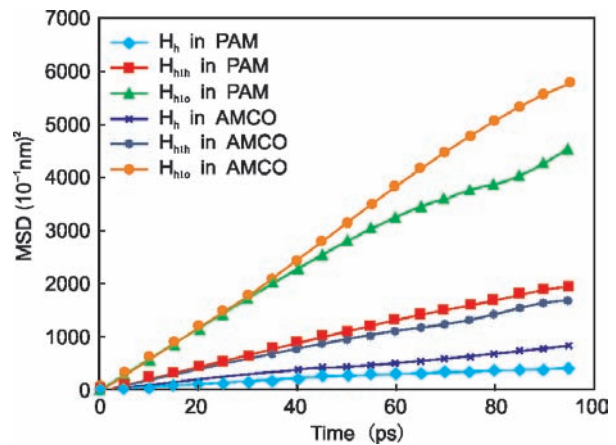


Fig. 9: MSD of hydrogen in aluminum melt

Table 3: Self-diffusion coefficient of hydrogen in aluminum melt

Melt	PAM			AMCO		
	h	h1h	h1o	h	h1h	h1o
Self-diffusion coefficient, $D(10^{-8}m \cdot s^{-1})$	0.91	3.62	9.03	1.59	3.31	10.31

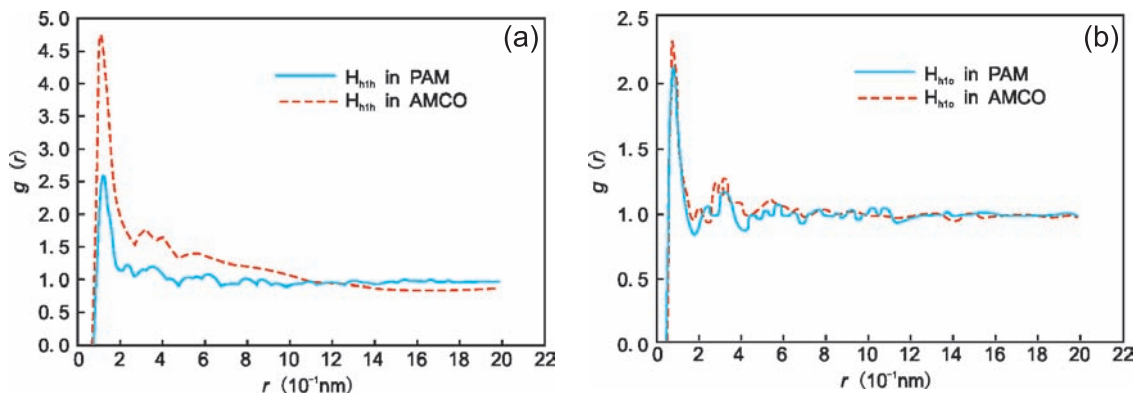


Fig.10: RDF curves of (a) H_{h1h} - H_{h1h} and (b) H_{h1o} - H_{h1o} in aluminum melt

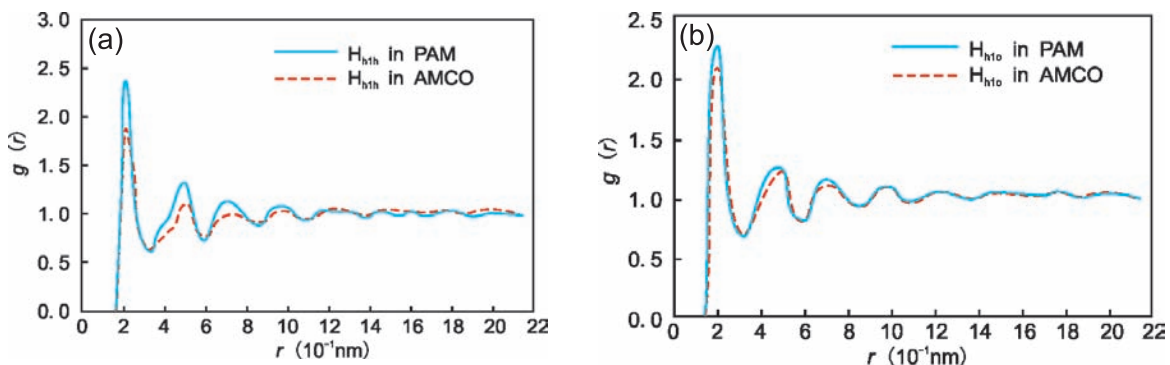


Fig. 11: RDF curves of (a) $Al-H_{h1h}$ and (b) $Al-H_{h1o}$ in aluminum melt

As shown in Fig. 10(a), the value $g(r)$ of the first peak in RDF curve of H_{h1h} - H_{h1h} is bigger than that of H_{h1o} - H_{h1o} [Fig. 10(b)], indicating that the aggregation of H_{h1h} is more significantly. Moreover, the coordination number N_{ij} of H_{h1h} is 0.21 and 0.59 in PAM and AMCO, respectively (Table 4), suggesting that the aggregation extent of H_{h1h} in AMCO should be deeper than that

in PAM. Similarly, the value N_{ij} of H_{h1o} in AMCO is a little bigger than that in PAM, meaning that Al_2O_3 accumulates H_{h1o} and decreases their dispersion slightly.

The values of r_{max} corresponding to the first peak in RDF curves are shown in Table 4, which reflect the distance between H atoms or ions that are affected by the hydrogen radius

Table 4: Main data of RDF curves

Data	PAM				AMCO			
	H _{h1h} -H _{h1h}	Al-H _{h1h}	H _{h1o} -H _{h1o}	Al-H _{h1o}	H _{h1h} -H _{h1h}	Al-H _{h1h}	H _{h1o} -H _{h1o}	Al-H _{h1o}
r _{max} (10 ⁻¹ nm)	1.21	1.95	0.77	1.79	1.09	1.97	0.79	1.79
Coordination number, N _i	0.21	0.37	0.08	0.35	0.59	0.39	0.092	0.34

and dispersion degree. The r_{max} value of dispersive H_{h1o} is the smallest, meaning the radius of H_{h1o} is the smallest. The influence of Al₂O₃ on r_{max} is slight for H_{h1o}, but it reduces H_{h1h} because of the decreasing dispersion degree shown in Fig. 8(b).

As presented in Fig.11, the value g(r) comes near 1 with the increase of value r, indicating that the distribution of H atoms or ions around Al atoms is in short-range order and long-range disorder. Furthermore, H_{h1o} is closer to Al atoms, and the distances between Al atoms and hydrogen are 0.179 nm for Al-H_{h1o} and 0.195 nm for Al-H_{h1h} (Table 4), leading to the detrimental effect in removal of H_{h1o}.

2.4 Discussion

The diffusion process of hydrogen is driven by van der Waals force which is expressed by Lennard-Jones 9-6 potential function shown as Eq. (3)^[30]:

$$U_{vdW}(r) = \sum \epsilon_{ij} \left[2 \left(\frac{r_{ij}^0}{r_{ij}} \right)^9 - 3 \left(\frac{r_{ij}^0}{r_{ij}} \right)^6 \right] \quad (3)$$

where r_{ij} is the distance of atom pairs and ε_{ij} is the potential well depth.

The van der Waals force includes attractive force and repulsive force in Fig. 12, and potential well depth ε reflects the attractive strength of atoms^[35]. The force field data of different types of hydrogen are shown in Table 5. Hydrogen diffuses into aluminum melt by interstitial atom. The smaller the radius of atom, the easier it is to diffuse. The radius of H_h is the biggest but the vacancies in aluminum melt are not big enough to accommodate them. Moreover, the potential well depth of H_h is the highest, which means the attractive force plays the key role in diffusion and makes H_h hard to diffuse. By comparison, H_{h1o} disperses in aluminum melt because its radius and potential well depth are both the lowest. The radius of H_{h1h} is close to H_{h1o}, whereas the potential well depth of H_{h1h} is close to H_h. From the above, the dispersion degree of H_{h1h} is between H_h and H_{h1o}. In addition, the diffusion process of H_{h1h} is easily affected by conditions around it. For example, Al₂O₃ cluster makes the ambient Al atoms array disordered [Fig. 2(b)] and creates more vacancies, which will attract H_{h1h} aggregation [Fig.8(b)] and cause the gas porosities to form in aluminum.

The interactions between Al₂O₃ and hydrogen have been studied by a great deal of experiments, and the results showed that the higher the Al₂O₃ concentration in aluminum melt, the more the hydrogen porosities, and Al₂O₃ inclusions act as the nucleation base of hydrogen gas^[4,9-11]. It can be concluded that gas porosities are mainly formed by H_{h1h} according to the simulation results. The H⁺ ions in aluminum melt are studied

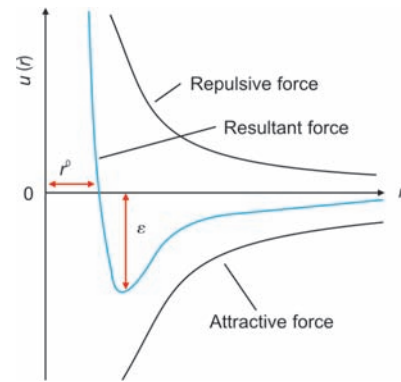


Fig.12: Lennard-Jones potential curves^[35]

Table 5: Force field data of different types of hydrogen^[30,37]

Hydrogen type	H _h	H _{h1h}	H _{h1o}
Atoms radius, r (Å)	1.2	0.37	0.25
Potential well depth ε (Å)	0.0230	0.0216	0.0080

rarely, but it was speculated that the adsorption of H atoms on Al₂O₃ generated contact potential which decomposed H atoms into H⁺ ions. The experiments on hydrogen removal by direct current showed that H⁺ ions transferred to cathode and transformed into H atoms and H₂ gas, which verified the existence of H⁺ ions in aluminum melt^[36]. The simulation results indicate that the removal of Al₂O₃ inclusions is important to eliminate gas porosities and the dispersive H⁺ ions must be removed by adsorption function of gas bubbles or molten fluxes.

3 Conclusions

(1) The adsorption areas in aluminum melts are maximums for H_{h1o} followed by H_{h1h} and H_h. H_h is hard to diffuse in aluminum melt and keep in cluster state. H_{h1h} and H_{h1o} both can diffuse easily, and H_{h1o} is more dispersive than H_{h1h} in aluminum melt. The radius and potential well depth cause the differences in diffusion for various types of hydrogen, and the smaller the radius and potential well depth of H atom, the easier it is to diffuse.

(2) Al₂O₃ cluster makes the ambient Al atoms disordered in aluminum melt and creates more vacancies to accumulate H_{h1h}, which causes the formation of gas porosities in aluminum. The simulation results agree well with the experimental findings, that is, the higher the Al₂O₃ concentration in aluminum melt,

the more the hydrogen porosities, and Al_2O_3 inclusions act as the nucleation base of hydrogen gas. The removal of Al_2O_3 inclusions is important for the elimination of gas porosities.

(3) H_{h10} is dispersive in aluminum melt and the distance of $Al-H_{h10}$ is shorter than that of other types of hydrogen, leading to detrimental effect to the removal of H_{h10} . Direct current degassing and adsorption of gas bubbles or molten fluxes are probably effective ways to remove dispersive hydrogen.

References

- [1] Anyalebechi P N. Analysis of the effects of alloying elements on hydrogen solubility in liquid aluminum alloys. *Scripta Metallurgica et Materialia*, 1995, 33(8): 1209–1216.
- [2] Alba-Baena N and Eskin D. Kinetics of ultrasonic degassing of aluminum alloys. *Light Metals*, 2013: 957–962.
- [3] Zeng Jianmin, Xu Zhengbing and He Juan. New process of elimination of hydrogen from melt aluminum. *Advanced Materials Research*, 2008, 51: 93–98.
- [4] Huang Liangyu and Yan Mingshan. Hydrogen in nonferrous metals and its alloys. Beijing: Metallurgical Industry Press, 1989: 157–164. (In Chinese)
- [5] Anyalebechi P N. Attempt to predict hydrogen solubility limits in liquid multicomponent aluminum alloys. *Scripta Materialia*, 1996, 34(4): 513–517.
- [6] Zeng J M, Tang L W and Lin S Y. Experimental study on hydrogen diffusion in molten aluminum. *Reviews on Advanced Materials Science*, 2013, 33: 257–260.
- [7] Lin R Y and Hoch M. The solubility of hydrogen in molten aluminum alloys. *Metallurgical Transactions A*, 1989, 20(9): 1785–1791.
- [8] Jiang Guangrui, Li Yanxiang and Liu Yuan. Calculation of hydrogen solubility in molten alloys. *Transactions of Nonferrous Metals Society of China*, 2011, 21(5): 1130–1135.
- [9] Li K D and Chang E. Mechanism of nucleation and growth of hydrogen porosity in solidifying A356 aluminum alloy: An analytical solution. *Acta Materialia*, 2004, 52(1): 219–231.
- [10] Bruna M, Sladek A and Kucharčík L. Formation of porosity in Al-Si alloys. *Archives of Foundry Engineering*, 2012, 12(1): 5–8.
- [11] Sigworth G K and Wang C. Mechanisms of porosity formation during solidification: A theoretical analysis. *Metallurgical Transactions B*, 1993, 24(2): 349–364.
- [12] Sabau A S and Viswanathan S. Microporosity prediction in aluminum alloy castings. *Metallurgical and Materials Transactions B*, 2002, 33(2): 243–255.
- [13] Carlson K D, Lin Z and Beckermann C. Modeling the effect of finite-rate hydrogen diffusion on porosity formation in aluminum alloys. *Metallurgical and Materials Transactions B*, 2007, 38(4): 541–555.
- [14] Zhang L, Lv X, Torgerson A T, et al. Removal of impurity elements from molten aluminum: A review. *Mineral Processing and Extractive Metallurgy Review*, 2011, 32(3): 150–228.
- [15] Roy R R, Utigard T A and Dupuis C. Inclusion removal kinetics during chlorine fluxing of molten aluminum. *Light Metals*, 2001: 991–997.
- [16] Warke V S, Shankar S and Makhlof M M. Mathematical modeling and computer simulation of molten aluminum cleansing by the rotating impeller degasser: Part II. Removal of hydrogen gas and solid particles. *Journal of Materials Processing Technology*, 2005, 168(1): 119–126.
- [17] Wu Ruizhi, Qu ZhiKun, Sun Baode, et al. Spray degassing as a method for hydrogen removal in aluminum melts. *Materials Transactions*, 2007, 48(5): 1029–1033.
- [18] Eskin D G. Ultrasonic processing of molten and solidifying aluminium alloys: Overview and outlook. *Materials Science and Technology*, 2016: 1–10.
- [19] Xua Hanbing, Jian Xiaogang, Meek T T, et al. Degassing of molten aluminum A356 alloy using ultrasonic vibration. *Materials Letters*, 2004, 58(29): 3669–3673.
- [20] Eskin D, Alba-Baena N, Pabel T, et al. Ultrasonic degassing of aluminium alloys: Basic studies and practical implementation. *Materials Science and Technology*, 2015, 31(1): 79–84.
- [21] Zeng Jianmin, Gu Ping and Wang Youbing. Investigation of inner vacuum sucking method for degassing of molten aluminum. *Materials Science and Engineering: B*, 2012, 177(19): 1717–1720.
- [22] Young G A and Scully J R. The diffusion and trapping of hydrogen in high purity aluminum. *Acta Materialia*, 1998, 46(18): 6337–6349.
- [23] Albrecht J, Bernstein I M and Thompson A W. Evidence for dislocation transport of hydrogen in aluminum. *Metallurgical Transactions A*, 1982, 13(5): 811–820.
- [24] Ulanovskiy I B. Hydrogen diffusion and porosity formation in aluminium. Moscow: National University of Science and Technology, 2015: 41–49.
- [25] Wang Zhaojing. Hydrogen and oxide inclusions in casting aluminium alloys. Beijing: Weapon Industry Press, 1989:26–34. (In Chinese)
- [26] Kang Jixing and Fu Gaosheng. The behaviors of inclusions and hydrogen in molten aluminium Special Casting and Nonferrous Alloys, 1995, 5: 5–8. (In Chinese)
- [27] Fu Gaosheng, Chen Wenzhe and Qian Kuangwu. Synthetical technique of high efficient melt treatment of aluminum and its effect. *The Chinese Journal of Nonferrous Metals*, 2002, 12(2): 269–274. (In Chinese)
- [28] Liu Yang, Dai Yongbing, Wang Jun, et al. Hydrogen diffusion in aluminum melts: An ab initio molecular dynamics study. *Journal of Wuhan University of Technology-Mater. Sci. Ed.*, 2012, 27(3): 560–567.
- [29] Liu Yang, Sun Baode, Dai Yongbing, et al. First principle study on hydrogen diffusion in degassing. *Key Engineering Materials*, 2011, 474: 1384–1387.
- [30] Sun H. Compass: An ab initio force-field optimized for condensed-phase applications overview with details on alkane and benzene compounds. *The Journal of Physical Chemistry B*, 1998, 102(38): 7338–7364.
- [31] Einstein A. On the movement of small particles suspended in stationary liquids required by the molecular-kinetic theory of heat. *Annalen der Physik*, 1905, 17: 549–560.
- [32] Mendez-Morales T, Carrete J, García M, et al. Dynamical properties of alcohol+1- Hexyl-3 - methyl imidazolium ionic liquid mixtures: A computer simulation study. *The Journal of Physical Chemistry B*, 2011, 115(51): 15313–15322.
- [33] Wang Ding, Tian Guocai. Simulation study of the effect of methanol on the structure and properties of 1-butyl-3-methyl imidazolium tetra fluoroborate ionic liquid. *Acta Physico-Chimica Sinica*, 2012, 28(11): 2558–2566. (In Chinese)
- [34] Solhjoo S, Simchi A and Aashuri H. Molecular dynamics simulation of melting, solidification and remelting processes of aluminum. *Transactions of Mechanical Engineering*, 2012, 36(M1): 13–23.
- [35] Jones J E. On the determination of molecular fields II. from the equation of state of a gas. *Proceedings of the Royal Society of London*, 1924, 106(738):463–477.
- [36] Li H, Zhang J, Liu X, et al. Research on the removal of hydrogen and sodium from Al-alloys melt by direct current. *Foundry*, 1995, 12: 1–4. (In Chinese)
- [37] Li C and Choi P. Molecular dynamics study of the adsorption behavior of normal alkanes on a relaxed α - Al_2O_3 (0001) surface. *Journal of Physical Chemistry C*, 2007, 111(4): 1747–1753.